Applied Surface Science 258 (2011) 1366–1372

Contents lists available at SciVerse ScienceDirect

Applied Surface Science

journal homepage: www.elsevier.com/locate/apsusc

Selective growth, characterization, and field emission performance of single-walled and few-walled carbon nanotubes by plasma enhanced chemical vapor deposition

Mihnea Ioan Ionescu, Yong Zhang, Ruying Li, Xueliang Sun*

Department of Mechanical and Materials Engineering, University of Western Ontario, London, ON N6A 5B9, Canada

ARTICLE INFO

Article history:
Received 21 June 2011
Received in revised form
13 September 2011
Accepted 15 September 2011
Available online 22 September 2011

Keywords:
Carbon nanotubes
Plasma enhanced chemical vapor deposition

ABSTRACT

Single-walled carbon nanotubes (SWCNTs) and few-walled carbon nanotubes (FWCNTs) have been selectively synthesized by plasma enhanced chemical vapor deposition at a relative low temperature (550 °C) by tuning the thickness of iron catalyst. The parametric study and the optimization of the nanotube growth were undertaken by varying inductive power, temperature, catalyst thickness, and plasma to substrate distance. When an iron film of 3–5 nm represented the catalyst thickness for growing FWCNT arrays, SWCNTs were synthesized by decreasing the catalyst thickness to 1 nm. The nanotubes were characterized by field emission scanning electron microscopy, transmission electron microscopy, and Raman spectroscopy. Electron field emission properties of the nanotubes indicate that the SWCNTs exhibit lower turn-on field compared to the FWCNTs, implying better field emission performance.

1. Introduction

Carbon nanotubes (CNTs) have drawn considerable attention for researchers due to their outstanding electrical, mechanical and optical properties [1–4] which lead to numerous applications of nanotubes as nanodevice components. Currently, various methods have been implemented to enable carbon nanotube synthesis such as arc discharge [5,6], laser ablation [7], and catalytic chemical vapor deposition [8]. The chemical vapor deposition (CVD) provides a reliable approach to grow nanotubes on different substrates and is suitable for scaled growth of high purity multi-walled and single-walled carbon nanotubes. In addition, CVD operates at substantially lower temperature than that in laser ablation and arc discharge processes [9].

In terms of applications of carbon nanotubes in semiconductor technology, vertically aligned CNTs exhibit potential applicability in electronics such as sensors [10,11], field emission devices [12], transistors, and logic circuits [13–15]. Therefore, in order to promote the development of nanotube devices integrated in silicon technology, it is essential to explore the synthesis and the assembly of vertical CNT arrays at low temperatures, on silicon substrates. Compared to the commonly used thermal chemical vapor deposition [16,17], plasma enhanced chemical vapor deposition (PECVD) presents significant advantages in terms of favouring vertically aligned growth of carbon nanotubes at low temperatures due to efficiency of precursor decomposition in the plasma sheath. Moreover, this procedure is compatible with the integrated circuits manufacturing process [18–20]. Despite successful development of PECVD using various plasma sources such as inductive coupled radio frequency, microwave, and direct current, there are still some issues to be addressed. Preventing the catalyst nanoparticles from agglomeration, maintaining the catalytic activity during the growth process, and abatement of ion damage to both catalyst nanoparticles and growing CNTs, are main requirements for PECVD methods [21–23]. One strategy in overcoming these problems is to generate plasma away from the substrate. This procedure reduces the plasma ion bombardment on the substrate and growing tubes [24]. However, detailed understanding of parametric effect on substrates exposed to the discharge is far from being achieved. Moreover, the reduction of synthesis temperature down to 500 °C is still a challenging task. Taking these into account and the fact that the inductive coupled plasma (IPC) sources can generate homogenous and stable plasma for uniform deposition, we proposed generating plasma away from the substrate for depositing vertically aligned carbon nanotubes (VA-CNTs). Recent studies have shown that CNTs have good electron field emission performances [25–27]. Many groups focused on vertically well-aligned multi-walled CNTs because of the difficulty to obtain well-aligned SWCNTs arrays. Moreover, previous comparisons of field emission for FWCNTs and SWCNTs are rare, most of which investigated field emission of MWCNTs and SWCNTs obtained by different synthesis procedures [28,29].

* Corresponding author. Fax: +1 519 661 3020.
E-mail address: xsun@eng.uwo.ca (X. Sun).

0169-4332/$ – see front matter © 2011 Elsevier B.V. All rights reserved.
doi:10.1016/j.apsusc.2011.09.065

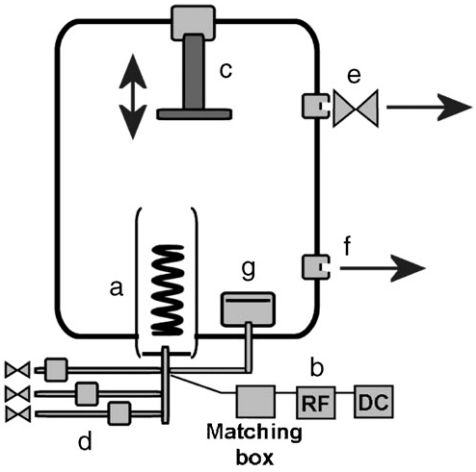

Fig. 1. Schematic diagram of PECVD deposition system – RF plasma source (a); matching box, and generators (b); substrate heating element with vertical movement (c); mass flow controller for gas inlets (d); connection to vacuum pump (e); connection to vacuum gauge (f); magnetron (g).

In this paper we have systematically investigated the effects of the growth parameters on CNT synthesis. By controlling the plasma conditions during the growth process, vertically aligned SWCNTs and FWCNTs have been selectively synthesized by tuning the thickness of catalyst at low substrate temperatures. Field emission properties of the SWCNTs and FWCNTs indicate that both types of the nanotubes are potential candidates for field emission applications, and the SWCNTs promise better field emission performance.

2. Experimental

The VA-CNTs were synthesized using the PECVD system schematically illustrated in Fig. 1. The plasma discharge source was controlled in inductively coupled mode and consisted of a copper coil wound around the outside of one inch quartz tube coupled with the feed-gas entrance (a). The inductive coil, powered by a 13.56 MHz RF generator (max 300 W), was connected to a matching network (b). The position of substrates along the axis of the quartz tube was set by a moving substrate holder. The substrates (up to 2 in. in diameter), attached to a resistive heating element, were placed at different distances from the plasma source by a vertical movement device (c). A thermocouple, implanted into the substrate holder, was used to calibrate and monitor the growth temperature. The assembly acted like a remote plasma reactor as no direct contact is between the plasma and the substrate. The system design allowed a minimum substrate to plasma distance of 8 cm. Mass flow controllers (d) were utilized to control the gas feeding directly into the plasma source. The deposition pressure was obtained by a vacuum pump (e), measured with a vacuum transducer (f), and controlled by either an electronic or a manual valve. For catalyst and/or under-layer material deposition the system was equipped with magnetron sputtering guns (g).

In this study, oriented n-type (1 0 0) silicon (Si) wafers were used as a substrate, without removing the native oxide layer. The reactor was continuously flushed with argon during loading and unloading of samples. The growth process could be divided into two main steps: the physical vapor deposition (PVD) of the catalyst followed by the PECVD growth of CNTs, without breaking the vacuum. In the first step, using magnetron sputtering, a 30 nm-aluminum (Al) under-layer was deposited on the Si substrate followed by sputtering iron (Fe) catalyst film. The thickness was monitored by a quartz crystal microbalance and the catalyst film was in the range of 0.5–7 nm. The aluminum film was used to effectively prevent the Fe catalyst particles from aggregation. For the second step, the pressure was increased to about 0.1 Torr and the substrate stage was heated up to the desirable temperature, allowing 10 minutes for temperature equilibration. Then the hydrogen–methane gas mixture (H_2:CH_4 = 1:11, total flow rate = 60 sccm) was admitted and the reactor pressure was set to 2 Torr. The inductive power to the coil was turned on, and plasma was ignited. After 15 min of growth time, the reactor was allowed to cool down under vacuum before exposure to air. For the optimization of growth conditions, one of the following parameters was varied while keeping the other parameters fixed. The optimum conditions were: 550 °C of the growth temperature, 200 W of the inductive power, and 10 cm of the substrate to plasma distance. The samples were characterized by scanning electron microscopy (SEM – Hitachi S-4800), Raman spectroscopy (Renishaw Raman spectrometer with laser excitation wavelength of 785 nm), and transmission electron microscopy (TEM – JEOL 2010F). The TEM samples were prepared by sonicating a small piece of as-grown nanotubes in ethanol for

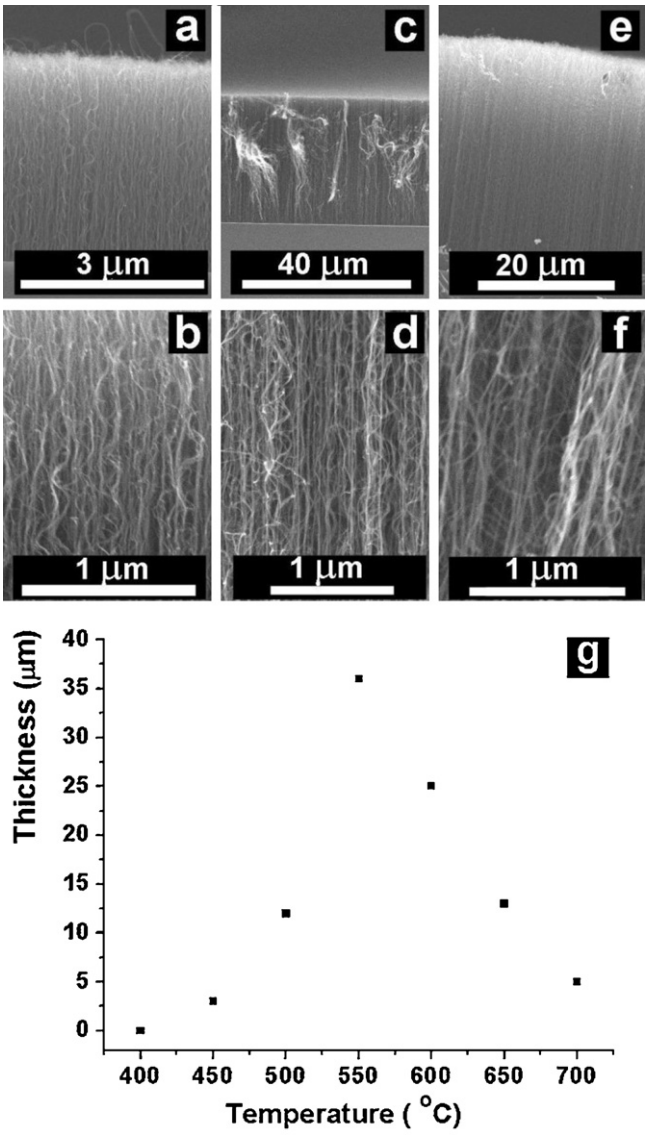

Fig. 2. SEM images of the CNTs obtained at 450 °C (low magnification) (a); 450 °C (high magnification) (b); 550 °C (low magnification) (c); 550 °C (high magnification) (d); 700 °C (low magnification) (e); 700 °C (high magnification) (f); illustration of the average tube length with temperature (g).

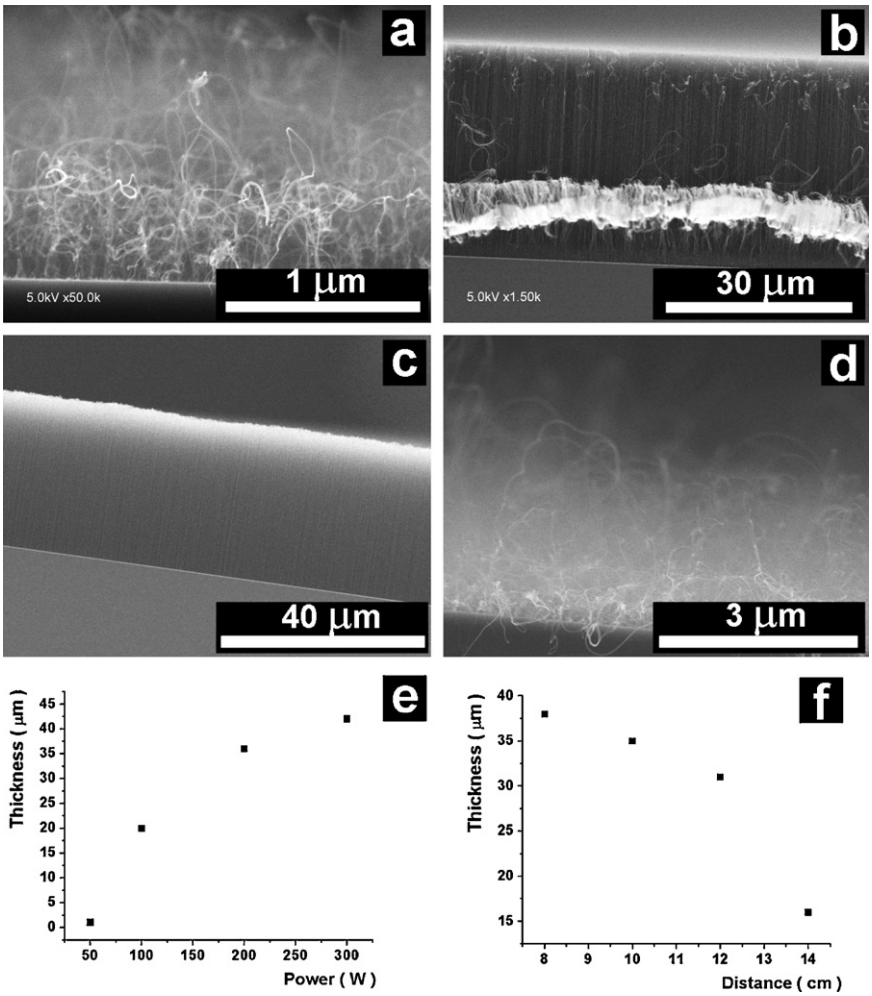

Fig. 3. SEM images of the CNTs obtained at 50 W plasma power (a) and 300 W (b); plasma to substrate distance of minimum 8 cm (c) and 16 cm (d). Plots of average nanotube length vs. plasma power (e) and substrate to plasma distance (f).

10 min and drying few drops of suspension on a Cu micro-grid. Field emission performance of the samples was studied in a vacuum system with a base pressure of 10^{-6} Torr. The field emission curves were obtained using a digital multimeter (Agilent 34410A). The measurements were carried out in a planar diode configuration with 34.2 mm^2 active area and with the anode to sample spacing of 200 μm. A glass plate, covered by a layer of indium-tin-oxide (ITO) thin film, was used as anode to collect the emitted electrons.

3. Results and discussion

The parametric study for this work evolved from efforts to obtain vertically oriented nanotubes with a narrow diameter distribution at relatively low temperatures. It involved perturbation of substrate temperature, plasma power, substrate distance, and catalyst thickness while keeping other parameters fixed as described in the experimental.

3.1. Influence of substrate temperature

In this study, nanotubes were grown at deposition temperatures in the range of 400–700 °C while all other parameters were kept constant. The plasma-heating effect could be ignored in these experiments, as the plasma was operated at moderate gas pressures [22] and large plasma to substrate distances. This aspect was verified by a thermocouple located directly under the sample holder. At 400 °C no deposit was found on the substrate. Fig. 2 shows SEM images for the nanotubes grown at 450 °C, 550 °C, and 700 °C respectively, for 15 min. The CNTs produced at 450 °C were vertically aligned, uniform in size, with a length of 3 μm (Fig. 2a and b). Compared with the results obtained at 550 °C (Fig. 2c and d), the tubes were much shorter, less dense, and larger in diameter. Considering the facts that no deposit occurred at 400 °C and plasma power was unchanged for these experiments, it suggests that hydrocarbon gas decomposed insufficiently on the substrate at temperature below 450 °C and the catalyst particle activity was too low to trigger the growth of CNT array [30].

The nanotubes grown at 550 °C were well-aligned and more uniform in diameter and height. The average tube length (Fig. 2g) presented a maximum of 36 μm at this temperature. When the deposition temperature was increased to 700 °C, the process of catalyst etching and agglomeration was accelerated. As a result, shorter CNTs were grown with twist morphology, more disorders, and poorer uniformity in size (Fig. 2e and f).

This systematic study demonstrated that quality VA-CNTs can be synthesized at relatively low temperatures. Even though the temperature as low as 450 °C was able to guarantee the achievement

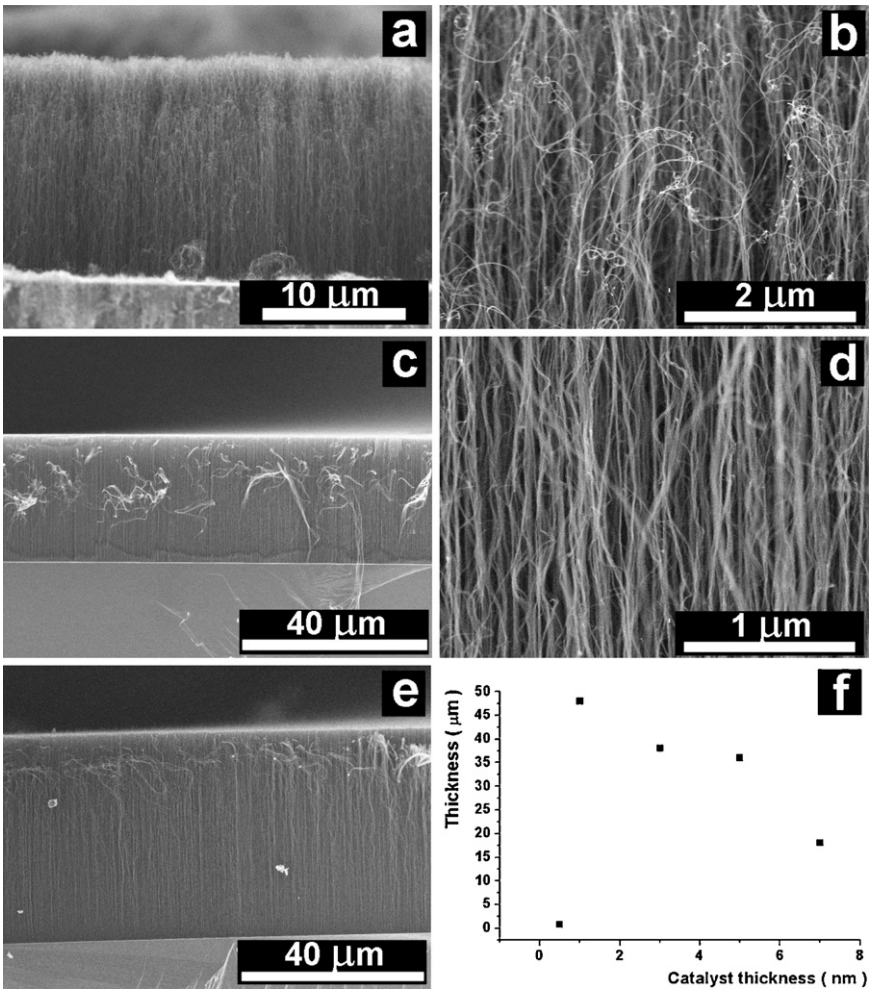

Fig. 4. SEM images of the carbon nanotubes grown using Fe catalyst with the thickness of 7 nm (a and b); 3 nm (c and d); 1 nm (e). A plot of CNT average thickness vs. catalyst thickness (f).

of CNT arrays, 550 °C was chosen as the optimum temperature in order to obtain well-aligned CNT arrays.

3.2. Influence of plasma power and substrate to plasma distance

Fig. 3 shows SEM images and schematic growth rate of the nanotubes under different plasma powers. It can be seen that the nanotube growth rate increases with increasing plasma power (Fig. 3a and b). This can be attributed to the fact that the increase of plasma power accelerated the decomposition of methane and, consequently, generated a larger amount of atomic hydrogen. In addition, the dehydrogenation of the adsorbed hydrocarbons and the carbon diffusion on the catalyst particles intensified and influenced the growth morphology [31–33]. At a low plasma power, less carbon species reacted with the catalyst particles to form nanotubes, reducing the growth rate, density, and alignment of CNTs (Fig. 3a).

The change of the distance between substrate and plasma had similar results (Fig. 3c and d). As shown in Fig. 3c, a short substrate to plasma distance of 8 cm produced long nanotubes. This growth was favoured by a high amount of atomic hydrogen and reactive carbon radicals in the proximity of catalyst surface. The atomic hydrogen made the catalyst particles active. By increasing the substrate to plasma distance to 16 cm, the carbon radicals formed in the plasma sheath recombined before reaching the catalyst particles, yielding insufficient growth, low density, and poor alignment of the nanotubes (Fig. 3d). Fig. 3e and f presents the average nanotube length as function of plasma power and substrate to plasma distance. The CNT length increased by intensifying the plasma power and by decreasing the substrate distance to plasma.

3.3. Influence of catalyst thickness

Size of catalyst particles has been shown to have a key role in controlling the tube diameter, length, and density in thermal CVD [34,35]. In order to examine the effect of catalyst film thickness on the morphology of CNT arrays, different initial thicknesses of Fe films, between 0.5 nm and 7 nm, were implemented in the nanotube growth. To diminish the ion bombardment effect over the substrate, the plasma power was set as 200 W and the substrate to plasma distance was located at 10 cm. SEM micrographs of nanotubes grown on 7 nm-thick Fe film reveal that the tubes are tangled and not densely packed (Fig. 4a and b). The wide diameter distribution can be attributed to the uneven fragmentation of the catalyst layer during the heating process [36].

By decreasing the catalyst film thickness to 3 nm and 5 nm, the tubes became longer, aligned, uniform in height and diameter, as shown in Fig. 4c and d. When the catalyst film thickness was down to 1 nm, thinner nanotubes were obtained with alignment and uniform size (Fig. 4e). However, the nanotubes were so thin and sensitive to the electron beam of SEM that they were not able to be clearly imaged at high magnification. Fig. 4f shows the influence of

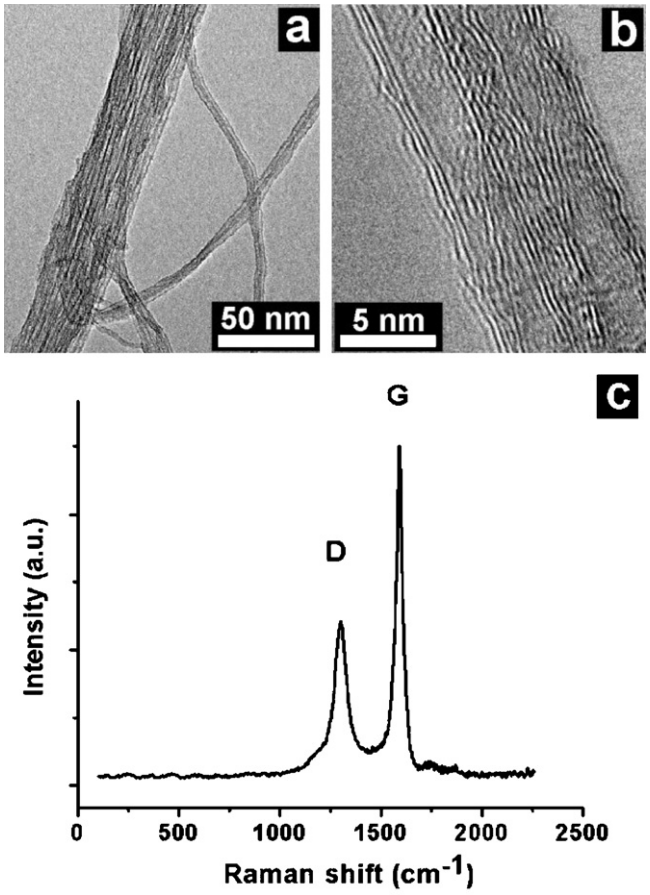

Fig. 5. Characterization of samples obtained for 3 nm catalyst thickness: low magnification TEM image of the FWCNT bundles (a); magnified TEM image of the FWCNTs (b); Raman spectrum of the FWCNTs (c).

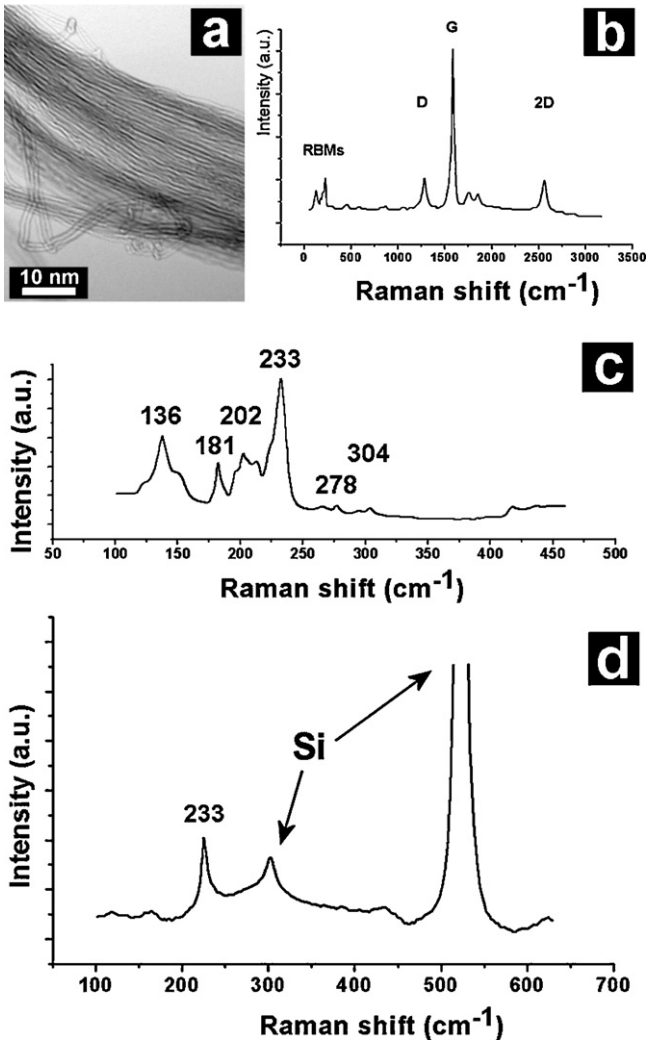

Fig. 6. Characterization of the samples obtained for 1 nm catalyst thickness: TEM image of the nanotube bundles (a); Raman spectrum (b); RBM region (c); RBM from a single bundle of the CNTs (d).

catalyst thickness on the length of the CNTs. Average CNT length increased by decreasing the catalyst thickness and reached a peak value (48 μm) when the thickness of Fe film was about 1 nm. For the catalyst film with the thickness of about 0.5 nm, no arrays were observed. The tubes were distorted and non-uniform in diameter. The suppression of CNT growth can be attributed to the reduced solubility of carbon in iron nanoparticles when the particle size is decreased [37]. It is also worth mentioning that no nanotube growth was observed in the absence of the catalyst film.

3.4. Structure characterization of FWCNTs and SWCNTs

A comprehensive investigation of the obtained nanotubes by TEM indicated that selective growth of FWCNTs and SWCNTs with uniform diameter could be realized by tuning the catalyst thickness based on optimized parameters. FWCNTs with outer diameter of 4–8 nm and inner diameter of about 2–5 nm could be obtained by using 3–5 nm thick iron catalyst layer, revealing relatively well defined graphitic shells parallel to the tube axis (Fig. 5a and b). The number of walls observed is in general between 3 and 6 walls.

Fig. 5c shows Raman spectrum of the FWCNTs, in which radial breath modes (RBMs) are absent and intensity of the D band relative to G band (I_D/I_G) is around 0.48. The disordered structure reflecting from the D band may originate from the defects and distortion of the graphene walls and from amorphous carbon on the nanotube surface. Fig. 6 presents TEM images and Raman spectrum of the nanotubes with 1 nm thick Fe catalyst. The presence of CNT bundles is clearly visible while the tubes present a narrow diameter distribution in the range of 1–2 nm. The tubes have even diameters and appear clean and uncoated with amorphous carbon. The Raman spectrum with a clearly visible RBM region (Fig. 6b) presents features related to a SWCNT spectrum. The RBMs (Fig. 6c) reveal that the majority of peak positions are between 136 and 233 cm^{-1}. These correspond to tube diameters of 1.85 and 1.05 nm [38], which are consistent with the TEM observations. The spectrum in Fig. 6d is acquired from a single bundle of nanotubes and shows an individual RBM peak at 233 cm^{-1}. This indicates a bundle of metallic-type SWCNTs. A lower I_D/I_G intensity ratio of 0.24 indicates a lower defect concentration within the SWCNTs compared to the FWCNTs. The results indicate that SWCNTs and FWCNTs can be selectively synthesized by tuning the catalyst thickness.

3.5. Field emission performance of FWCNTs and SWCNTs

The field emission properties of CNTs were measured using the substrate coated with as grown nanotubes as cathode. For this study FWCNTs obtained for 3 nm catalyst thickness and SWCNTs obtained for 1 nm catalyst thickness have been used. The correlation of current density versus electric field of the FWCNTs and SWCNTs is shown in Fig. 7 along with liner Fowler-Nordheim plots, indicating field emission behavior of both types of the nanotubes. The turn-on field, defined as the field under which a 10 μA cm^{-2} current density is extracted [25], was determined to be 0.417 V μm^{-1} and

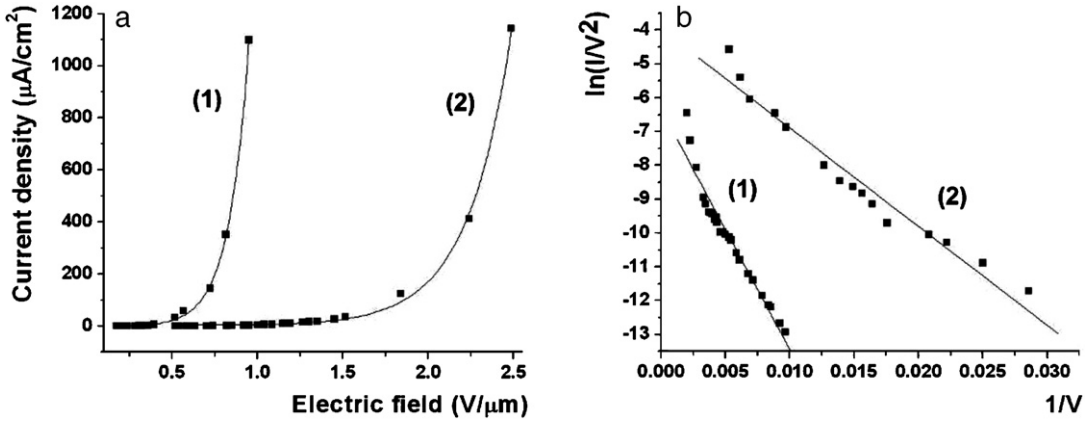

Fig. 7. Curves of current density vs. electric field and Fowler–Nordheim plots for the SWCNTs (curve (1)) and for FWCNTs (curve (2)).

1.237 V μm^{-1} for SWCNTs and FWCNTs, respectively. The current density of 1 mA/cm^2, required for most conventional flat panel displays, was determined to be achieved at field levels of 2.458 V μm^{-1} for FWCNTs and even at lower field levels of 0.938 V μm^{-1} for SWCNTs. These findings imply that the obtained SWCNTs exhibit superior emission properties than the FWCNTs, and are in concordance with previous reports [28,29].

Fig. 7b shows Fowler–Nordheim plots of the nanotubes. Fowler–Nordheim (F–N) equation is used as a mathematic interpretation of field emission for carbon nanotube arrays:

$$\ln\left(\frac{J}{E^2}\right) = \ln\left(\frac{A\beta^2}{\phi}\right) - \frac{B\phi^{3/2}}{\beta E} \quad (1)$$

where J is the field emission current density in A cm^{-2}, E is the applied electric field in V cm^{-1}, and ϕ is the work function of emitters in eV. The constants $A = 1.54 \times 10^{-6}$ A eV V^{-2} and $B = 6.83 \times 10^9$ eV$^{-3/2}$ V m^{-1} are derived from quantum statistics. The applied electrical field E is proportional to the local electrical field (E_{loc}) and related to the applied voltage (V) by setting $E_{loc} = \beta E = \beta V/d$, where d is the distance between anode and cathode and β is the enhancement factor. The field enhancement factor is related with the slope (S_{FN}) of F–N plots, $\beta = -B\phi^{3/2}/S_{FN}$, and depends on the geometry and surface properties of CNT emitters [39]. As seen from the above TEM and Raman characterizations, defects and larger diameter of the FWCNTs have an impact on the geometry and radius curvature of field emitter tips. Moreover, SWCNTs have a lower defect concentration and are grown in bundles of smaller diameter tubes providing additional emission sites. The linear F–N plots indicate a smaller slope for SWCNTs caused by a larger field emission β factor than that for FWCNTs. The slope of F–N equation is also proportional to the work function of emitters ϕ, which might be another reason for the differences in emission properties between FWCNTs and SWCNTs. Unfortunately, precise values of the work functions for different types of CNTs are not yet known. Further research work is necessary to quantify the difference between the FWCNTs and SWCNTs.

4. Conclusions

Vertically aligned carbon nanotubes have been synthesized at relatively low temperature using an inductive coupled PECVD system. A parametric study of the nanotube growth has been carried out to investigate the effect of the involved factors on the nanotube growth, such as substrate temperature, plasma power, substrate to plasma distance, and catalyst thickness. VA-CNTs have been successfully synthesized at temperatures as low as 450 °C. FWCNTs and SWCNTs can be selectively obtained by tuning the catalyst thickness from 3–5 nm to 1 nm. The electron field emission measurement and calculation of the nanotubes indicates that the SWCNTs exhibit better field emission characteristics than the FWCNTs and their performances recommend both nanomaterials for field emission applications.

References

[1] M.S. Dresselhaus, G. Dresselhaus, P.C. Eklund, Science of Fullerenes and Carbon Nanotubes, Academic Press, San Diego, 1996.
[2] R. Saito, G. Dresselhaus, M.S. Dresselhaus, Physical Properties of Carbon Nanotubes, Imperial College Press, London, 1998.
[3] J. Bernholc, D. Brenner, M.B. Nardelli, V. Meunier, C. Roland, Mechanical and electrical properties of nanotubes, Annu. Rev. Mater. Res. 32 (2002) 347–375.
[4] A. Jorio, G. Dresselhaus, M.S. Dresselhaus, CarbonNanotubes Advanced Topics in the Synthesis, Structure, Properties and Applications, Springer, Berlin, 2008.
[5] S. Iijima, T. Ichihashi, Single-shell carbon nanotubes of 1-nm diameter, Nature 363 (1993) 603–605.
[6] C. Journet, W. Maser, P. Bernier, A. Loiseau, M. Lamy de la Chapelle, S. Lefrant, P. Deniard, R. Lee, J. Fischer, Large-scale production of single-walled carbon nanotubes by the electric-arc technique, Nature 388 (1997) 756–758.
[7] A. Thess, R. Lee, P. Nikolaev, H. Dai, P. Petit, J. Robert, Chunhui Xu, Young Hee Lee, Seong Gon Kim, A. Rinzler, D. Colbert, G. Scuseria, D. Tombnek, J. Fischer, R. Smalley, Crystalline ropes of metallic carbon nanotubes, Science 273 (1996) 483–487.
[8] J. Kong, A.M. Cassell, H. Dai, Chemical vapor deposition of methane for single-walled carbon nanotubes, Chem. Phys. Lett. 292 (1998) 567–574.
[9] A.M. Cassell, J.A. Raymakers, J. Kong, H. Dai, Large scale CVD synthesis of single-walled carbon nanotubes, J. Phys. Chem. B 103 (1999) 6484–6492.
[10] J. Kong, N.R. Franklin, C. Zhou, M.G. Chapline, S. Peng, K. Cho, H. Dai, Nanotube molecular wires as chemical sensors, Science 287 (2000) 622–625.
[11] T. Yamada, Y. Hayamizu, Y. Yamamoto, Y. Yomogida, A. Izadi-Najafabadi, D.N. Futaba, K. Hata, A stretchable carbon nanotube strain sensor for human-motion detection, Nat. Nanotechnol. 6 (2011) 296–301.
[12] D.H. Lee, J.A. Lee, W.J. Lee, S.O. Kim, Flexible field emission of nitrogen-doped carbon nanotubes/reduced graphene hybrid films, Small 7 (2010) 95–100.
[13] T. Rueckes, K. Kim, E. Joselevich, G.Y. Tseng, C.L. Cheung, C.M. Lieber, Carbon nanotube-based nonvolatile random access memory for molecular computing, Science 289 (2000) 94–97.
[14] H.W.C. Postma, T. Teepen, Z. Yao, M. Grifoni, C. Dekker, Carbon nanotube single-electron transistors at room temperature, Science 293 (2001) 76–79.
[15] H. Ryu, D. Kalblein, R.T. Weitz, F. Ante, U. Zschieschang, K. Kern, O.G. Schmidt, H. Klauk, Logic circuits based on individual semiconducting and metallic carbon-nanotube devices, Nanotechnology 21 (2010) 475207.
[16] K. Hata, D.N. Futaba, K. Mizuno, T. Namai, M. Yumura, S. Iijima, Water-assisted highly efficient synthesis of impurity-free single-walled carbon nanotubes, Science 306 (2004) 1362–1364.
[17] V.K. Kayastha, S. Wu, J. Moscatello, Y.K. Yap, Synthesis of vertically aligned single- and doublewalled carbon nanotubes without etching agents, J. Phys. Chem. C 111 (2007) 10158–10161.
[18] Y. Li, D. Mann, M. Rolandi, W. Kim, A. Ural, A. Javey, J. Cao, D. Wang, E. Yenilmez, Q. Wang, J. Gibbons, Y. Nishi, H. Dai, Preferential growth of semiconducting single-walled carbon nanotubes by a plasma enhanced CVD method, Nano Lett. 4 (2004) 317–321.
[19] G. Zhong, T. Iwasaki, K. Honda, Y. Furukawa, I. Ohdomari, H. Kawarada, Very high yield growth of vertically aligned single-walled carbon nanotubes by point-arc microwave plasma CVD, Chem. Vapor Depos. 11 (2005) 127–130.
[20] M.J. Behr, E.A. Gaulding, K.A. Mkhoyan, E.S. Aydil, Effect of hydrogen on catalyst nanoparticles in carbon nanotube growth, J. Appl. Phys. 108 (2010) 053303.

[21] G. Zhang, D. Mann, L. Zhang, A. Javey, Y. Li, E. Yenilmez, Q. Wang, J. McVittie, Y. Nishi, J. Gibbons, H. Dai, Ultra-high-yield growth of vertical single-walled carbon nanotubes: hidden roles of hydrogen and oxygen, Proc. Natl. Acad. Sci. U.S.A. 102 (2005) 16141–16145.
[22] Z. Luo, S. Lim, Y. You, J. Miao, H. Gong, J. Zhang, S. Wang, J. Lin, Z. Shen, Effect of ion bombardment on the synthesis of vertically aligned single-walled carbon nanotubes by plasma-enhanced chemical vapor deposition, Nanotechnology 19 (2008) 255607.
[23] M. Meyyappan, A review of plasma enhanced chemical vapour deposition of carbon nanotubes, J. Phys. D: Appl. Phys. 42 (2009) 213001.
[24] S. Alexandrov, Remote PECVD: a route to controllable plasma deposition, J. Phys. IV: France 5 (1995) 567–582.
[25] J. Bonard, J. Salvetat, T. Stockli, W. de Heer, L. Forro, A. Chatelain, Field emission from single-wall carbon nanotube films, Appl. Phys. Lett. 73 (1998) 918–920.
[26] Y. Yang, C. Wang, U. Chen, W. Hsieh, Y. Chang, H. Shin, Large-area single wall carbon nanotubes: synthesis, characterization, and electron field emission, J. Phys. Chem. C 111 (2007) 1601–1604.
[27] P. Hojati-Talemia, G.P. Simon, Enhancement of field emission of carbon nanotubes using a simple microwave plasma method, Carbon 49 (2011) 484–486.
[28] A. Wadhawan, R. Stallcup, K. Stephens, J. Perez, I. Akwani, Effects of O2, Ar, and H2 gases on the field-emission properties of single-walled and multiwalled carbon nanotubes, Appl. Phys. Lett. 79 (2001) 1867–1869.
[29] S. Boddepalli, S. Boddepalli, K. Noh, M. Jeon, W. Choi, Enhanced field emission from aligned multistage carbon nanotube emitter arrays, Nanotechnology 19 (2008) 065605.
[30] A. Gohier, T. Minea, M. Djouadi, J. Jimenez, A. Granier, Growth kinetics of low temperature single-wall and few walled carbon nanotubes grown by plasma enhanced chemical vapor deposition, Physica E 37 (2007) 34–39.
[31] Y. Chen, L.P. Guo, D.J. Johnson, R.H. Prince, Plasma-induced low-temperature growth of graphitic nanofibers on nickel substrates, J. Cryst. Growth 193 (1998) 342–346.
[32] P.E. Nolan, D.C. Lynch, A.H. Cutler, Carbon deposition and hydrocarbon formation on group VIII metal catalysts, J. Phys. Chem. B 102 (1998) 4165–4175.
[33] D. Hash, M. Meyyappan, Model based comparison of thermal and plasma chemical vapor deposition of carbon nanotubes, J. Appl. Phys. 93 (2003) 750–752.
[34] M. Chhowalla, K.B.K. Teo, C. Ducati, N.L. Rupesinghe, G.A.J. Amaratunga, A.C. Ferrari, D. Roy, J. Robertson, W.I. Milne, Growth process conditions of vertically aligned carbon nanotubes using plasma enhanced chemical vapor deposition, J. Appl. Phys. 90 (2001) 5308–5317.
[35] M. Bell, K. Teo, W. Milne, Factors determining properties of multi-walled carbon nanotubes/fibres deposited by PECVD, J. Phys. D: Appl. Phys. 40 (2007) 2285–2292.
[36] Z. Tsakadze, I. Levchenko, K. Ostrikov, S. Xu, Plasma-assisted self-organized growth of uniform carbon nanocone arrays, Carbon 45 (2007) 2022–2030.
[37] A.R. Harutyunyan, N. Awasthi, A. Jiang, W. Setyawan, E. Mora, T. Tokune, K. Bolton, S. Curtarolo, Reduced carbon solubility in Fe nanoclusters and implications for the growth of single-walled carbon nanotubes, Phys. Rev. Lett. 100 (2008) 195502.
[38] M. Dresselhaus, G. Dresselhaus, R. Saito, A. Jorio, Raman spectroscopy of carbon nanotubes, Phys. Rep. 409 (2005) 47–99.
[39] S.K. Srivastava, V.D. Vankar, V. Kumar, Excellent field emission properties of short conical carbon nanotubes prepared by microwave plasma enhanced CVD process, Nanoscale Res. Lett. 3 (2008) 25–30.